Journal of Carcinogenesis
Covering Genesis to Therapeutics

Journal of Carcinogenesis, ISSN: 1477-3163
2025; Vol 24: Issue 5s, https://carcinogenesis.com/

Cable Condition Diagnosis of Induced voltage and Sheath Current Monitoring

Priya Selvamany[1], Jayashree Ramasubramanian[*2], R. Sundar[3]

[1,*2]Department of Electrical and Electronics Engineering, B.S. Abdur Rahman Crescent Institute of Science and Technology, Vandalur, Chennai -600048, India

Email ID: priya.gdv@gmail.com

[3]Department of Marine Engineering, AMET Deemed to be University, Chennai-603112, (sundar.r@ametuniv.ac.in

***Corresponding Author:**

Jayashree Ramasubramanian

Email ID: jayashree@crescent.education

ABSTRACT

An integrated system for monitoring the condition of high voltage (HV) power cables and localizing faults is proposed. The methodology focuses on identifying faults in the cable sheath by analyzing sheath system currents in underground cable systems. The approach begins with the development of a numerical model to simulate sheath currents. Following this, the paper presents an analysis of various common and consequential faults based on current measurements at the link cable. Simulations of both normal and fault conditions are provided to assess the feasibility of fault detection. To model a faulted underground cable system, an equivalent circuit is analyzed using a lumped parameter approach. This model allows for the examination of radial configurations of metallic cable sheath grounding and their effect on the induced voltages within the sheath. By modeling and analyzing the monitored sheath currents and induced outer sheath voltage, the fault finding can be determined. Finally, case studies are presented, evaluating the system's performance with varying fault distances and resistances. These evaluations highlight the system's effectiveness in fault localization and condition monitoring.

Keywords: *Sheath current; induced voltages; fault location; underground power cable; electric breakdown; cable shielding*

How to Cite: Priya Selvamany, Jayashree Ramasubramanian, R. Sundar, (2025) Cable Condition Diagnosis of Induced voltage and Sheath Current Monitoring , *Journal of Carcinogenesis*, *Vol.24, No.5s*, 826-836

1. INTRODUCTION

Underground cables are commonly used due to concerns about reliability and the environment. To enhance the reliability of a distribution system, accurately identifying the faulted segment is crucial for minimizing service interruption time. This allows for a quicker restoration of service by promptly pinpointing the faulted segment. Traditional fault detection methods involve conducting an exhaustive search over large distances, which is both time-consuming and inefficient. Moreover, this approach wastes manpower and may result in varying restoration times depending on the reliability of outage information. Therefore, developing an efficient technique for fault location can significantly improve system reliability. Locating a faulted segment in an underground cable system requires a comprehensive approach involving various considerations and analyses [1]. In contrast to overhead lines, underground cables exhibit lower inductance and higher capacitance. The analysis becomes more complex when multiple types of underground cables are involved. An example of this would be a cable system that includes multiple conductors, such as the core, sheath, and armor. When analyzing such a cable system, mutual impedances and admittances between the conductors must be considered in the circuit analysis. This adds complexity to the task of identifying the fault location. Generally, fault location techniques for underground cable networks can be divided into two categories: 1) Tracer and 2) Terminal. The tracer method is a thorough approach to locating a faulted segment by "walking" through the cable circuits [2]. A faulted segment can be identified through audible or electromagnetic signals, which necessitates dispatching crew members to the outage area. Various techniques are widely used in the industry, including the tracing method, which relies on acoustic, electromagnetic, or current-based approaches [3]. In contrast, the terminal method is a technique used to determine the fault location of a distribution cable network from one or both ends, without the need for exhaustive tracing. One of the most used terminal methods is the bridge technique, which uses a resistor to identify the fault location [4]. The traveling wave approach is another method

for detecting faults by injecting pulse signals into a defective cable. This generates reflected waveforms that can be used to identify the fault [5-7]. Similarly, fault generated waves have been used to perform both real-time and after the fact fault location for residential distribution cable systems in single-phase configuration [8-10]. Field engineers experience suggests that a significant number of cable failures are caused by excessive sheath current. These failures can result from issues such as flooded cable joints, corrosion, third-party damage to the cable jacket, and breakdown of insulation between the cable sheaths at both ends of a cable joint [11-13]. Mingzhen Li et al. have developed a method to detect and localize faults in CB configurations through the monitoring of sheath currents [14]. Cross-linked polyethylene (XLPE) is used as an insulation material in high-temperature superconducting cables, where repeated pulse voltages, often caused by lightning strikes and commutation failures in high-voltage DC systems, can lead to significant issues [15]. Xiang Dong et al. [16] developed various criteria, based on the type of defect, to detect faults in cable sheaths by measuring sheath currents without transposition are used in a flat formation. The estimation of fault distance is based on voltage and current measurements taken at the sending end.

Therefore, in this work, the effects of pulse voltage method are implemented on the current and voltage characteristic of the multi-section cables have been analyzed. The analysis is carried over to quantitatively measure the induced sheath voltage and rise in ground potential in the fault portion, which depends on insulation fault resistance. This study suggests using sheath system currents as indicators for detecting cable sheath faults. The results will afford guidance and helpful for determining the insulation condition and to prevent premature failure of cables by taking prompt action.

2. STRUCTURE OF UNDERGROUND CABLE

2.1 The Cable configuration

Figure 1 illustrates the symmetrical positioning of the three-phase single-core coaxial cable and its cross-section, where the core and sheath serve as the inner and outer conductors, respectively. The cables are buried at specific depths beneath the earth's surface, which results in a higher capacitance compared to overhead lines. A simulation has been conducted for a 400 kV HV cable circuit with a cross-sectional area of 2500 mm². The specifications and parameters of the cross-sectional structure are provided in Tables 1 and 2. In Figure 1b, the directions of both voltages and currents are clearly illustrated, with the phase ‘R’ cable.

Table 1. Specifications of the cable.

Parameters	Radius(mm)	Thickness (mm)
Core	a=17.9	-
Inner semiconducting screen	b=18.9	1
XLPE main insulation	c=29.9	11
Outer semiconducting screen	d=30.9	1
Aluminum outer sheath	e=31.2	0.3

Table 2. Parameters of the cable.

Parameters	Values
Inductance per unit length	0.5456μH/m
Capacitance per unit length	235pF/m
Resistance per unit length	1.023μΩ/m
Insulation conductance per unit length	5.4779e-15 S/m
Line length	300m
Permittivity of the insulation	2.3

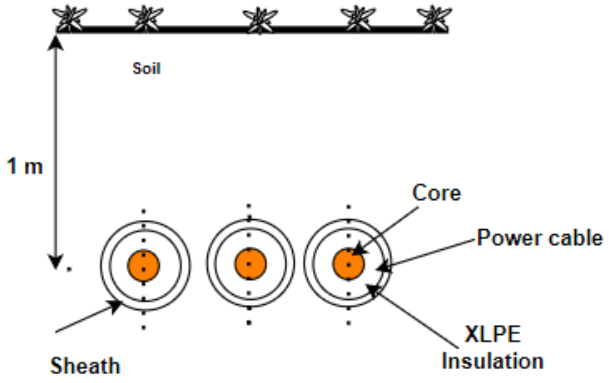

Figure 1a. Three phase 400kV, single-core XLPE Cable

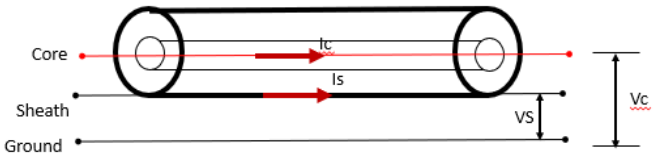

Figure 1b. Voltage and current representation on phase 'R' cable

2.2 CABLE SYSTEM model

Figure 2 illustrates a connection network of HV cable section. Each of the three phases consists of three minor sections. At both ends of the major section, the terminals or joints are connected to other cable sections, overhead lines, or substation equipment. The metal sheaths at both ends of the major section are directly grounded through the grounding boxes, G1 and G2. Within the major section, the cable joints J1, J2, serve to connect the different minor sections. Coaxial link cables are used to connect the metal sheaths to the link boxes, where cross-bonded connections are implemented within the link boxes, J1 and J2. The metal sheaths at both ends of a major section are directly grounded through the grounding boxes. Within the major section, cable joints are used to connect different minor sections. The core conductors of each phase are directly linked through cable joints, while the metal sheaths are connected to the link cables. These link cables connect the sheaths to the link boxes, where the cross-bonded connections are established inside the link boxes. The online condition monitoring system requires the installation of current transformers (CTs) [17]. It should be noted that the current measured at each CT includes both leakage currents (calculated as the phase voltage divided by the insulation impedance) and the sheath circulating current, which results from the imbalance of induced voltages within the sheath loop.

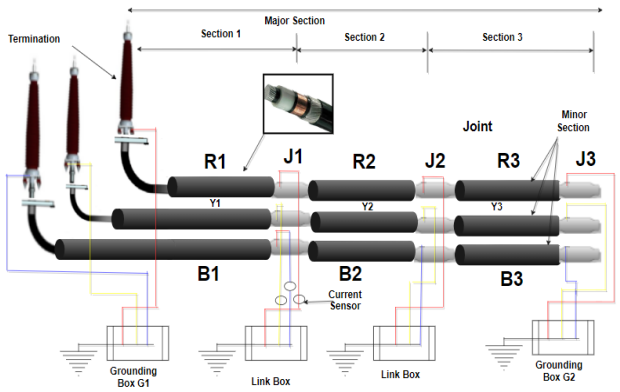

Figure 2. The configuration of a single-core HV cable system connection.

2.3 PERFORMANCE EVALUATION FOR MULTI-SECTION CABLE

Due to the implementation of the multiple-point grounding method on the shields, the cable line is modeled in multiple segments, with the length of each segment varying according to the configuration. An equivalent circuit model for a Single-Line-to-Ground (SLG) fault is established, which includes a set of unknown circuit parameters. The voltage and current determination at the fault point, as shown in Figure 3, is given by the following expression:

The lumped parameter approach for the underground cable system is represented in multiple sections, owing to the application of the multiple-point grounding method. It is assumed that a core-to-sheath-to-ground fault occurs in one of the phases (for instance, phase-R), as illustrated in Fig. 2. The cable model can be simplified as a two-port network, as depicted in Fig. 3b. The equivalent network can be represented by two transfer function matrices [17]: the transfer function matrix H and the admittance matrix Y_c, as given in Equation (1) [18].

$$Y_c V_j - I_j = 2H^T I_{kr} = 2I_{ji}$$
$$Y_c V_k - I_k = 2H^T I_{ji} = 2I_{ki} \quad (1)$$

Here, H and Y_c are defined by Equations (2) and (3), respectively.

$$H = e^{-\sqrt{ZY}.l} \quad (2)$$
$$Y_c = Z^{-1}\sqrt{ZY} \quad (3)$$

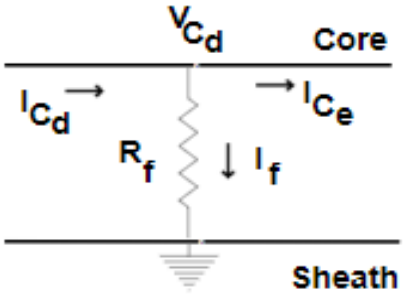

Figure 3a. Representation of core-to-sheath to ground fault

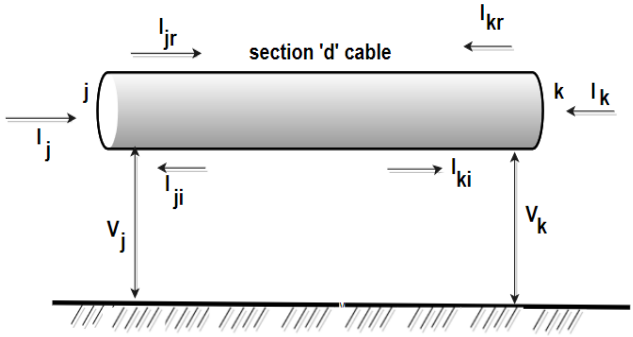

Figure 3b.Two -port network of the cable

Where Z and Y represent the series impedance and shunt admittance per unit length, respectively; l is the cable length; V_j and V_k are the voltage vectors at nodes j and k; I_j and I_k are the current vectors at nodes j and k; I_{jr} and I_{kr} are the reflective current vectors at nodes j and k. Equations (1) to (3) imply that H and Y_c represent the transmission characteristics, with Z and Y. The fundamental equations describing a transmission line system are provided in Equations (4) and (5) [18].

$$\frac{dV}{dx} = -zI \quad (4)$$

$$\frac{dI}{dx} = -Y.V \quad (5)$$

Each section of the cable is 300 meters in length, resulting in a total length of 3000 meters. Section 'd' extends from the sending end to the fault point, while section 'i' spans from the fault point to the receiving end, with the load connected at section 'm'. The fault current flows through the fault resistance to the earth. At both ends of each single-section cable, two

grounding resistances (R_g) are connected to the sheath for every 300 meters are shown in figure 4a.

3. FAULT CASES UNDER STUDY

In this study, there are two fault locations, which are under consideration.

- Fault at third section (section‘f’).
- Fault at midway in cable model (section ‘h’).

Pulse voltage tests for the given cases have been carried out with varying fault distance and fault resistance. The fault distances range from 900m to 3000m, and the fault resistances considered are 0.1Ω, 15Ω, 50Ω, and 100Ω. The estimated results show that the sheath current, ground current, ground potential, and core-sheath fault voltage are significantly influenced by changes in fault resistance.

3.1 TEST ON CABLE NETWORK REPRSENTATION WITH EARTH RETURN path

The circuit shown in Fig. 4 illustrates the grounding sheath distance and its connection to the faulted point. The case study, as depicted in Fig. 4a, represents a multi-section cable system consisting of ten sections. This simulation model is designed with a shorter length to assess the effectiveness of the proposed fault location. In this case study, a Single Line-to-Ground (SLG) fault in phase A is assumed, involving both the core and sheath. The system operates at a voltage level of 10 kV, with a rise time of 20μs and a fall time of 2ms, while the total length of the cable is 3 km. The sheath grounding resistance is set to 10 ohms, and the load impedance is defined as Z_L=324+j156.9037 Ω. The cable configuration parameters used in this case study are provided in Table II. The system's performance has been tested for accuracy by varying both the fault distance and fault resistance.

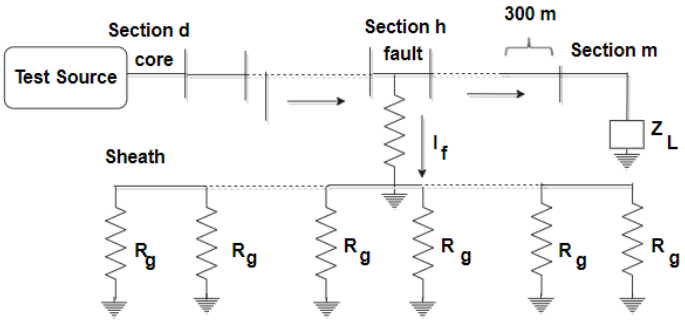

Figure 4a. Case setup for Multi-section cable system

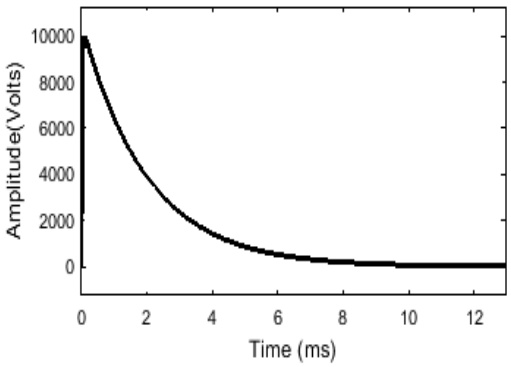

Figure 4b. Applied pulse voltage signal.

3.2 EVALUATION OF inDUCED SHEATH VOLTAGE

This study discusses the induced voltages in the concentric metallic sheaths of high voltage power cables. The magnitude of these voltages primarily depends on factors such as the length, construction, and configuration of the cables. In practice, the sheaths of high voltage cables can operate with various bonding methods, including single-point bonding, both-ends bonding, and cross bonding. In this study, the induced sheath voltages are analyzed for a 400 kV underground power transmission system, which consists of three single core cables. The permissible touch voltage U_{Tp} (curve 1) and

permissible prospective touch voltages U_{vTp} (with added resistances in earth path- curves 2, 3, 4, 5) as a function of time in high voltage substations are presented in figure 5 [19]. For times exceeding 10 seconds, if there are no additional resistances in the earth path, the permissible touch voltage U_{Tp} is set to 80 V. This value is considered representative in the given scenario. The configuration of the cables and sheaths is deemed acceptable when the induced voltages do not exceed 80 V. The analysis of the induced sheath voltages was carried out using MATLAB software. The sheath voltages and load currents in the cable conductors were calculated for the configurations mentioned earlier. In the first test case configuration, the induced voltage was found to be relatively low across all the cable sheaths between the distances of 300m to 600m and 1200m to 2700m. The permissible voltage value of 80 V is slightly exceeded in the sheath of section 'l' for a fault resistance of 100Ω and in the sheath of section 'm' for fault resistances of 50Ω and 100Ω, respectively. The highest induced sheath voltage values are observed with a fault resistance of 50Ω in section 'l', where the voltage exceeds by 11.46%, and with a fault resistance of 100Ω in section 'm', where it exceeds by 31.25% as shown in Figure 6. These values are considered unacceptable. However, this fault resistance configuration is not suitable for an ended section cable. In this study, we assume that the fault occurs between sections 'e' and 'g', which is referred to as section 'f'. The construction of a single-core xlpe underground cable is modeled using the lumped parameter pi-model, specifically developed for multi-section systems, to evaluate its performance and explore the potential of the pulse voltage technique. A comparison was made using various fault resistances in XLPE insulated cables, with their characteristics discussed in this section. It is important to note that the sheath circulating current is caused by the imbalance of the induced voltages in the sheath loop.

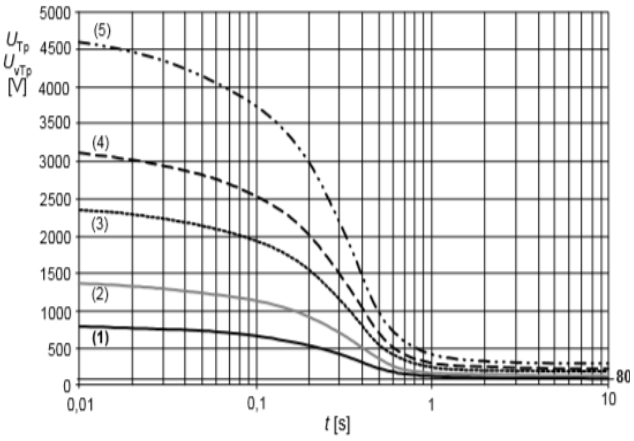

Figure 5. Permissible touch voltage [19]

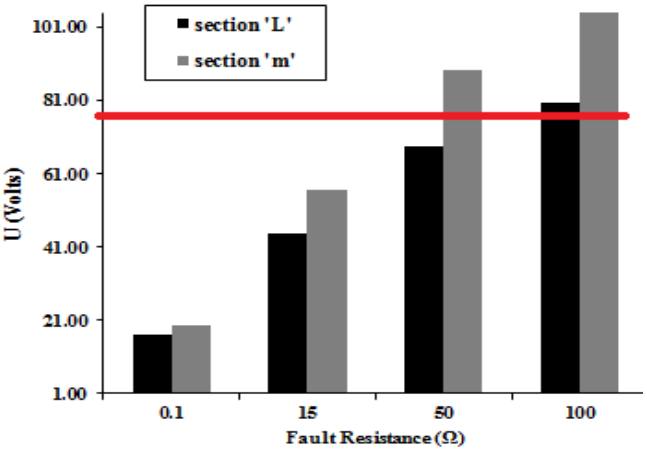

Figure 6. Cables configuration in Test I cases; U – analysed sheath-to-earth voltage

Taking section 'f' as an example, if a single-phase short circuit fault occurs in this section, the fault current in the center conductor on the source side would be high, while the current on the load side would be nearly 0 A. Figure 7 shows that a high core-to-sheath fault voltage of 6.63 kV is observed in the faulted section 'f' of the cable configuration for a fault resistance of 100Ω. This results in a significantly lower voltage at the ground potential, measured at 336.1 volts at a 300m length. In contrast, the induced voltage at the 2700m and 3000m lengths from section 'd' is much lower compared to the other sections.

Meanwhile, the ground potential in section 'f' shows a higher voltage of 955.2 volts for a fault resistance of 0.1Ω. The simulation results of the ground potential at each detection point are presented in Figure 8. It is observed that as the fault resistance increases, the ground potential across all sections rises monotonically. However, the greatest increase in potential is observed at the load termination section 'm' relative to the fault section.

3.3 CONDITION DIAGNOSIS OF HV CABLE SHEATH current

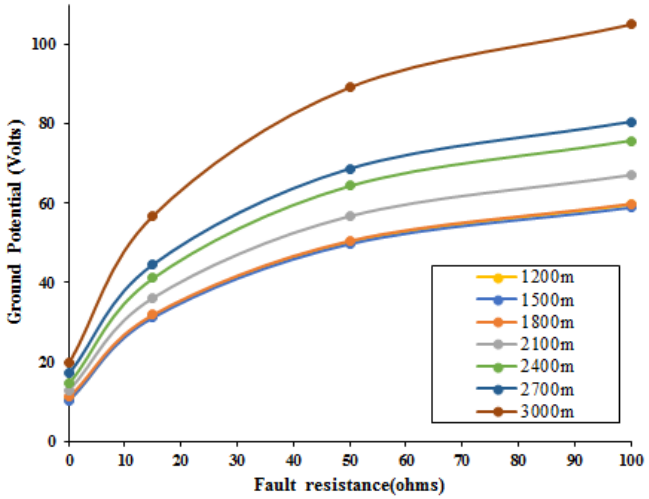

Figure 8. Detected ground potential with different fault resistance

Excessive current in the sheath can cause overheating of the cable insulation, leading to a reduced lifespan or even thermal breakdown of the insulation and cable joints. Additionally, the sheath current also includes leakage current, which can provide valuable information about the condition of the main cable and joint insulation. Any significant degradation in the main insulation would result in increased dielectric loss (DL) [25].

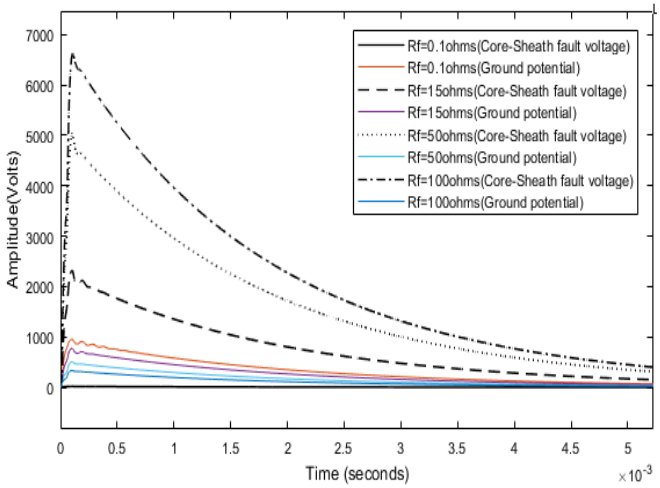

Figure 7. The detected induced sheath voltage and ground potential for different fault resistance at section 'f' (Test case –I).

Sheath current can be utilized for cable fault localization. This study proposes using the sheath circulating current as an indicator to monitor the relative dielectric loss among the three-phase cables, aiding in the assessment of the condition of the cable's outer sheath. Leakage current plays a crucial role in calculating dielectric losses (DL), as it represents the current flowing through the insulation when the cable is operating under voltage [26].

The leakage current offers insights into the condition of the insulation, but the interconnection of the sheaths makes interpretation challenging. Transmission and distribution cable systems are often installed in the same duct or tunnel, with their sheaths connected to the same earth terminal due to limited grounding space. Figure 9 demonstrates how leakage currents flow through the insulation and into the earth for various fault resistances. However, the currents detected at the ground also include leakage currents from the fault sections, which follow the same trend as the sheath

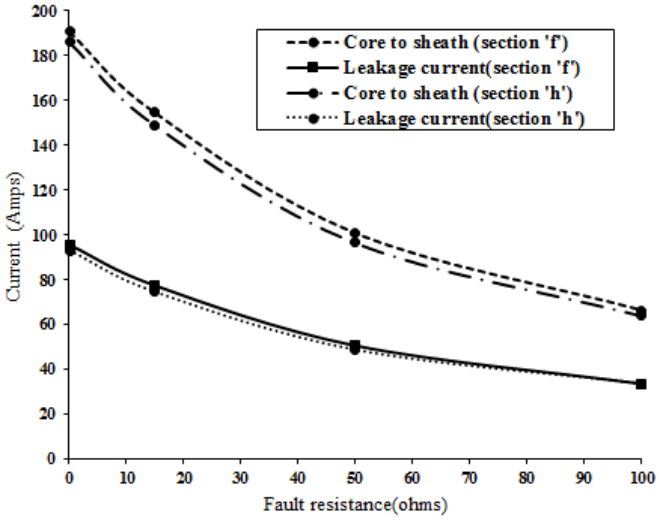

Figure 10. Variation of core to sheath and leakage current by comparing two fault locations.

current.

Figure 10 presents the measurements of sheath current and leakage current for two test cases. The first case involves a fault at the third section, while the second case involves a fault at the middle section. Both cases show that as the fault resistance increases, both currents gradually decrease. Consequently, a relatively high circulating sheath current of approximately 190.9A is observed for a fault resistance of 0.1Ω, while the detected currents at 100Ω are around 66.39A.

Evidence indicates that the electrical cycling, combined with the expansion of the cable, is significant enough to cause wear and damage to the outer sheath. As the cable experiences these mechanical abrasions, the protective lead sheath undergoes a process known as work hardening, where the material becomes stiffer, less malleable, and has reduced ductility. Over time, this leads to the development of fatigue cracks and voids, which ultimately reduce the lifespan and effectiveness of the lead sheath. Once moisture enters through the cracked sheath, it begins to degrade the dielectric properties of the insulation[27-28].

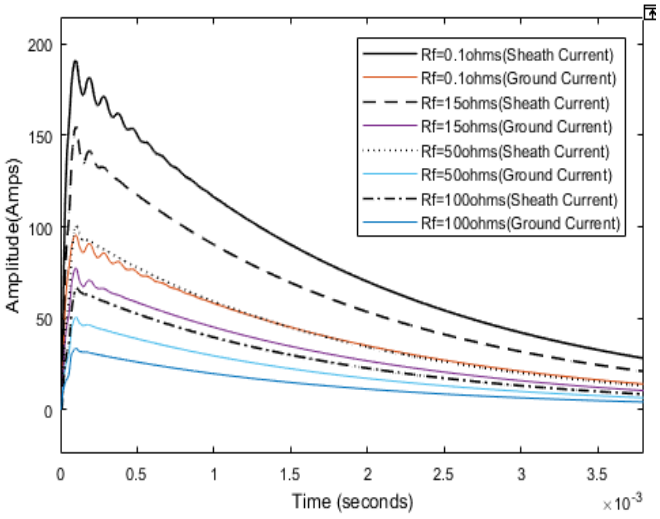

Figure 9. Core -to-Sheath and Leakage current measurement with fault resistance variation

As observed in Figure 11, the cable configurations in both test cases show that the injected source current decreases as the fault resistance varies. Additionally, the core currents in sections ‘g’ and ‘i’ gradually increase with increasing fault resistance. Figure 12 further demonstrates that, when a single-phase fault occurs, the core current response increases in proportion to the fault resistance. This suggests that it is reasonable to determine the fault section by analyzing the fundamental signal of the sheath leakage currents to ground. Therefore, maintaining a healthy sheath is crucial for power cables, especially for high voltage single-core cables, to ensure their optimal performance and longevity.

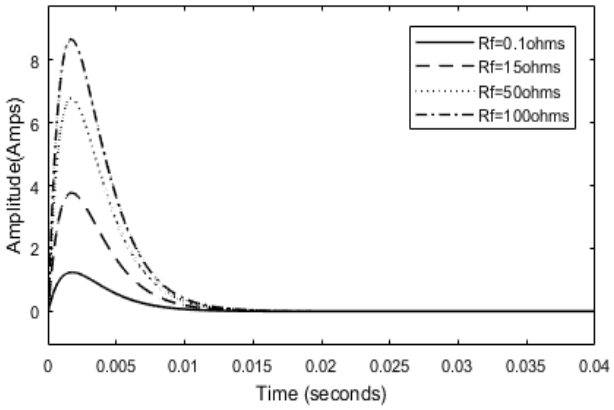

Figure 12. Output current response for fault occurred at section 'f (Test case –I).

Although improvements were made, Figure 13 still shows some deviation in the leakage current along the length of the cable. The results for Test Case I demonstrate the use of sheath-to-ground currents as indicators to detect cable sheath faults. For selected values of Rf, the simulated resistive faults at a distance dr=900 m along a cable section of length l=3000 m. The obtained currents related to the sheath, resistances, and the distance from the fault point were compared. The average reduction rate of the sheath current was 23.32% for a 15Ω fault,

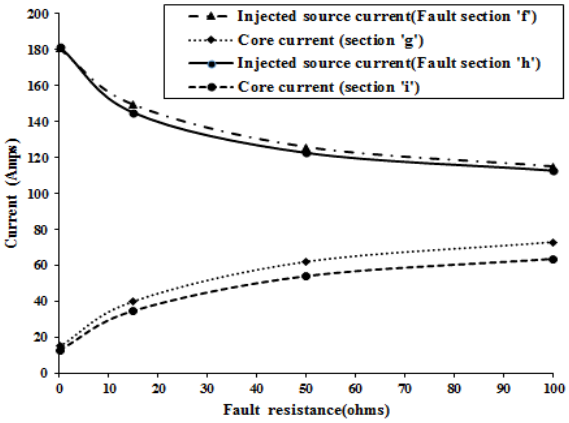

Figure 11. The results of current (Test case –I and II).

approximately 88.62% for 50Ω, and 184.2% for 100Ω, when compared to a 0.1Ω fault resistance. As a result, the difference in sheath-to-ground current is more significant when a 100Ω fault resistance occurs compared to the core-to-sheath current. It is important to note that the earth return currents are accounted for, and complete shielding is not assumed in this analysis. It is important to note that earth return currents are considered, and complete shielding is not assumed. The differences between the fault and non-fault conditions arise from the variations in the equivalent circuit and the cable impedance per unit length. These differences are primarily due to the changes introduced by the presence of a short-circuit fault, which affects the electrical connections and coupling between the cable conductors and the cable sheaths.

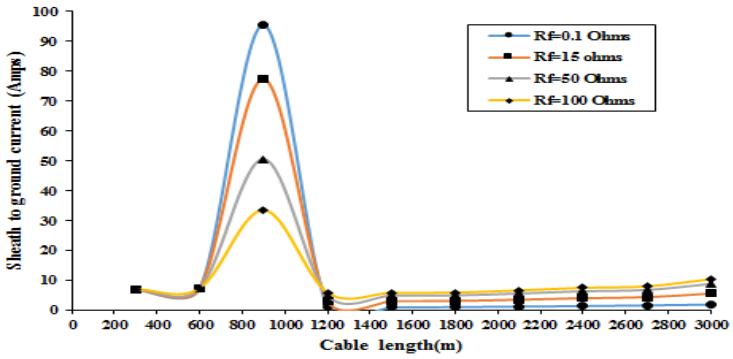

Figure 13. Variation of sheath to ground current with cable length (Fault occurred at section 'f', Test case –I).

4. CONCLUSIONS

The pulse voltage technique has been investigated in this study to analyze the induced sheath voltage, rise in electrical potential, and ground current characteristics. These factors are quantitatively compared under varying fault resistance conditions, which are indicative of degradation in XLPE cables. The following observations have been made:

(i) Induced sheath voltages are influenced by the method of bonding and the location of earthing of the cable sheaths.

(ii) For the analyzed power transmission system, which includes varying fault resistance in cables per phase, a higher resistance fault, such as 100Ω, in the cable configuration results in the highest level of induced voltage.

(iii) The use of sheath currents for condition monitoring of HV power cables enables trending analysis of dielectric loss, assessment of the cable sheath systems' condition, and rapid fault localization.

This work emphasis the pulse voltage technique study is valuable and great significance for the diagnosis of cable in the future. Further research will expand to include the transposition of cables.

Conflicts of Interest

The authors declare that they have no conflicts of interest.

REFERENCES

[1] Shijun Yi et al: “A regulatory approach to the assessment of asset replacement in electricity networks”, Asset Management Conference 2011, IET, London

[2] L. M. Wedepohl, and D. J. Wilcox, “Transient analysis of underground power-transmission systems System-model and wave-propagation characteristics” PROC. IEE, Vol.120, No. 2, pp. 253-260, 1973.

[3] E. C. Bascom, “Computerized underground cable fault location exper- tise,” in Proc. IEEE Power Eng. Soc. General Meeting, Apr. 10–15, 1994, pp. 376–382.

[4] E. Bungay and D. Macllister, Electric Cable Handbook, 2nd ed. Ox- ford, U.K.: BSP, 1990.

[5] T. Tanaka and A. Greenwood, Advanced Power Cable Technology. Boca Raton, FL: CRC, vol. 1.

[6] L. M. Wedepohl, H.V. Nguyen, and G.D. Irwin, “Frequency-Dependent Transformation Matrices for Untransposed Transmission Lines using Newton-Raphson Method”, IEEE Transactions on Power Systems, Vol. 11, No. 3, pp. 1538-1546, 1996

[7] J.-H. Sun, “Fault location of underground cables using travelling wave,” KIEE Trans., pp. 1972–1974, Jul. 2000.

[8] S. Potivejkul, P. Kerdonfag, S. Jamnian, and V. Kinnares, “Design of lowvoltagecablefaultdetector,”inProc.IEEEPowerEng.Soc.Winter Meeting, Jan. 2000, vol. 1, pp. 724–729.

[9] C. M. Wiggins, D. E. Thomas, T. M. Salas, F. S. Nickel, and H.-W. Ng, “A novel concept for urd cable fault location,” IEEE Trans. Power Del., vol. 9, no. 1, pp. 591–597, Jan. 1994.

[10] J. Moshtagh and R. K. Aggarwal, “A new approach to fault location in a single core underground cable system using combined fuzzy logic and wavelet analysis,” in Proc. 8th IEEE Int. Conf. Developments in Power System Protection, 2004, Apr. 2004, vol. 1, pp. 228–231.

[11] M.-S. Choi, S.-J. Lee, D.-S. Lee, and B.-G. Jin, “A new fault location algorithm using direct circuit analysis for distribution systems,” IEEE Trans. Power Del., vol. 19, no. 1, pp. 35–41, Jan. 2004.

[12] M.-S. Choi, D.-S. Lee, and X. Yang, “A line to ground fault location algorithmforundergroundcablesystem,”KIEETrans.PowerEng.,pp. 267–273, Jun. 2005.

[13] W. A. Thue, Electrical Power Cable Engineering, 2nd ed. Boca Raton, FL: CRC, 2003.

[14] Mingzhen Li, W. Zhou, Chunlin Wang, Leiming Yao, Mengting Su, Xiaojun Huang and C. Zhou, "A novel fault localization method based on monitoring of sheath current in a cross-bonded HV cable system", 2017 IEEE Electrical Insulation Conference (EIC), 2017.

[15] B. X. Du and L. W. Zhu ,’ Electrical Tree Characteristics of XLPE under Repetitive Pulse Voltage in Low Temperature’, IEEE Transactions on

[16] Dielectrics and Electrical Insulation Vol. 22, No. 4; August 2015, pp.1801-1808. DOI 10.1109/TDEI.2015.005183

[17] L. H. Becker, J. H. Cloete, and H. C. Reader, “Radio frequency coupling between an antenna and two unshielded parallel wires above a metal sheet-measurement precautions,” IEEE Trans. Electromagn. Compat., vol. 43, no. 1, pp. 85–88, Feb. 2001.

[18] W. H. Kersting, Distribution System Modeling and Analysis, 1st ed. Boca Raton, FL: CRC, 2001.

[19] Xia Yang, Student Member, IEEE, Myeon-Song Choi et al., “Fault Location for Underground Power Cable

[20] Using Distributed Parameter Approach”, IEEE Transactions on Power Systems, Vol. 23, No. 4, November 2008,pp. 1809-1816

[21] Stanislaw Czapp et al,” Induced sheath voltages in 110 kV power cables – case study”, Archives of Electrical Engineering, Vol. 64(3), pp. 361-370 (2015). DOI 10.2478/aee-2015-0028

[22] J. Barrett and G. Anders. Circulating current and hysteresis losses in screens, sheaths and armour of electric power cables — mathematical models and comparison with IEC Standard 287. IEE Proceedings - Science, Measurement and Technology, 1997, 144(3): 101-110.

[23] X. Dong, Y. Yuan, Z. Gao, C. Zhou: "Analysis of cable failure modes and cable joint failure detection via sheath circulating current", IEEE Electrical Insulation Conference (EIC), Philadelphia, USA, IEEE: 2014, 294-298.

[24] Orton H.: "Power cable technology review". High Voltage Engineering, 2015, 41(4): 1057-1067.

[25] X. Peng, C. Zhou, D.M. Hepburn, M. Judd and W.H. Siew: “Application of K-Means Method to pattern Recognition in On-line Cable PD Monitoring”, IEEE Transactions on Dielectrics and Electrical Insulation, June, 2014

[26] Bojie Sheng, Chengke Zhou et al: PD localisation in cross-bonded 3- phase HV cable systems. IEEE trans. DEIS, Oct. 2104

[27] Yang Yang, Donald M. Hepburn, Chengke Zhou: "On-line Monitoring and Trending Analysis of Dielectric Losses in Cross-bonded High Voltage Cable Systems", Jicable, 2015.

[28] Duan, D.P; Zeng,Y.; Huang, C.J; Sheng, G.H., Digital algorithm based on orthogonal decomposition for measurement of dielectric loss factor, Generation, Transmission and Distribution, IET, Vol: 2, No: 6, Nov, 2008.

[29] M. Marzinotto and G. Mazzanti. The Feasibility of Cable Sheath Fault Detection by Monitoring Sheath-to-Ground Currents at the Ends of Cross-Bonding Sections. IEEE Transactions on Industry Applications, 2015, 51(6): 5376-5384.

[30] Bjorn Gustavsen, Adam Semlyen, “Combined Phase and Modal Domain Calculation of Transmission Line Transients Based on Vector Fitting”, IEEE Transactions on Power Delivery, Vol. 13, No. 2, pp. 596-604, 1998.